JOURNAL OF SOLID STATE CHEMISTRY 92, 57–67 (1991)

Chemical Pressure and Other Effects of Strontium Substitution in $YBa_2Cu_3O_{9-\delta}$

P. KAREN, H. FJELLVÅG, AND A. KJEKSHUS

Department of Chemistry, University of Oslo, Blindern, N-0315 Oslo 3, Norway

AND A. F. ANDRESEN†

Institute for Energy Technology, N-2007 Kjeller, Norway

Received September 28, 1990; in revised form December 4, 1990

High quality samples of the $Y(Ba_{1-y}Sr_y)_2Cu_3O_{6.948(6)}$ solid solution phase were prepared via citrate gels by mixing the components on an atomic level. The range of solid solubility is $0.00 \leq y \leq 0.35(3)$ for a 910°C firing temperature and constant oxygen content, as determined by iodometry. At standardized conditions, the limiting phase with $y = 0.35(3)$ is in equilibrium with $Y_2(Ba_{0.9}Sr_{0.1})CuO_5$ and $(Sr,Y)_{14}Cu_{24}O_{41}$, and the situation is described in terms of a tetrahedral four-component phase diagram. The slightly enhanced (anisotropic) contraction along the c axis of the unit cell, observed upon introduction of the smaller Sr atoms, is associated with apical compression of the coordination square pyramids of copper. Both the volume contraction and its anisotropy can be compared with the effects of applied pressure. In terms of chemical pressure $P^* = \varepsilon \cdot y$, coefficients of $\varepsilon_V = 6.8(2)$ GPa or $\varepsilon_{D_t} = 2.4(4)$ GPa are obtained, depending on whether ε is deduced from unit cell volume V or its (tetragonal) distortion D_t. The responses of the superconducting state upon the applied and chemical pressure (the latter exerted at the Ba site) are, however, quite different, with $\Delta T_c/\Delta P = 0.7$ K/GPa and $\Delta T_c/\Delta y = -20(2)$ K. A specific feature must hence either be introduced by the real pressure (e.g., increase in carrier concentration) or by the chemical pressure [e.g., local strain effects and/or redistribution of oxygen around Cu(1) site].

Introduction

The effects of pressure on the properties of superconductors are frequently studied (*1*) as valuable experiments to test theoretical models of superconductivity and to facilitate further insight into the phenomenon. In particular, the variation of T_c with pressure shows a striking diversity (*2–4*) for different high-T_c superconductors, which calls for explanation. Chemical simulation of pressure effcts is a valuable, additional tool in the process of resolving this situation. In the structure of the 90 K, high-T_c superconductor, $YBa_2Cu_3O_{9-\delta}$, the Ba site is a potential candidate for pressure modelling through chemical substitution. Although the Ba site lies within the layered Cu–O covalent network (the metric of which is altered by the substitution), the electronic structure at the key Cu sites is likely to be virtually preserved.

A comparison of ionic radii for Ba^{2+} and Y^{3+} shows that some potential substituents may tend to replace yttrium as well. Of the candidates (Na^+, Ca^{2+}, Sr^{2+}, Nd^{3+}, Pr^{3+},

† Deceased.

0022-4596/91 $3.00

and La^{3+}), only Sr^{2+} and La^{3+} were found (*5–7*) to substitute solely for barium, leaving the Y site intact. Since introduction of La^{3+} would induce an undesirable additional alteration, either in the oxygen content or in the amount of charge carriers (*8, 9*), strontium substitution seems to be the best candidate for chemical modelling of pressure effects. Relatively many reports (*10–19*) discuss superconductivity in the Sr-substituted phase. However, the available information is impaired by the lack of oxygen content data, which are crucial for T_c, and few details are found about the variation of interatomic distances in $Y(Ba_{1-y}Sr_y)_2Cu_3O_{9-\delta}$ over the entire solid solution region.

In this paper, the Sr for Ba substitution is reexamined in the frame of the Y(O)–Sr(O)–Ba(O)–Cu(O) phase diagram. Crystal structure data of $Y(Ba_{1-y}Sr_y)_2Cu_3O_{9-\delta}$ are reported, as refined from neutron and X-ray powder diffraction data. The substitution-induced contraction of the unit cell is compared with the effects produced by external pressure, and T_c is correlated with interatomic distances.

Experimental

Synthesis. The samples were prepared by firing of precursor materials obtained by liquid mixing in citrate gels. The starting components, viz., Y_2O_3 (5N, Megon), $SrCO_3$ (5N, Koch-Light), $BaCO_3$ (reagent grade, Merck) and $CuCO_3 \cdot Cu(OH)_2 \cdot 0.5H_2O$ (puriss., Riedel de Häen), were dissolved in boiling citric acid monohydrate (reagent grade, Fluka) to form a clear, blue, gel-like solution. The citrate gel was dehydrated at 180°C, finely milled, and incinerated in air at 450°C. The obtained powder was pressed into pellets and repeatedly fired at 910°C for 20 hr and at 340°C for 16 hr (intermediate cooling rate 120°C/hr) in a corrundum boat placed inside a tube furnace. The furnace was continuously flushed with oxygen gas purified on CuO at 600°C and on KOH at ambient temperature. Three intermittent rehomogenizations were performed, the last one being only coarse crushing in order to ensure full oxygen saturation.

Oxygen analyses. The oxygen content was determined iodometrically by thiosulfate titrations. The analyzed iodine was obtained from oxidation of iodide solution by, respectively, the sample as such and by a sample prereduced by HCl. The use of finely milled samples, ultrasound agitation, and inert atmosphere ensured a reproducible and quantitative course of the solid–liquid reaction, while additions of NH_4SCN and soluble starch enhanced the accuracy of the titration. The reproducibility is ± 0.005 in units of the formal oxidation state of copper.

Powder X-ray diffraction (PXD). All samples were characterized by PXD, using Guinier Hägg cameras, $CuK\alpha_1$ radiation, and Si as internal standard. Positions and integrated intensities of Bragg reflections were obtained by means of a Nicolet L18 film scanner and the SCANPI program system (*20*). Unit cell dimensions were deduced by least square refinements (*21*) including only unambiguously indexable lines.

Powder neutron diffraction (PND). Neutron diffraction diagrams were obtained on the two-axis diffractometer OPUS III at the JEEP II reactor, Kjeller. Monochromatic neutrons of wavelength 187.7 pm were used, and diffraction data were collected in steps of $\Delta 2\theta = 0.05°$ between $2\theta = 5°$ and 100°.

Least squares refinements were carried out according to the Rietveld method (*22*) using the Hewat version (*23*) of the program. The scattering lengths $b_Y = 7.75$, $b_{Ba} = 5.25$, $b_{Sr} = 7.02$, $b_{Cu} = 7.72$, and $b_O = 5.81$ fm were used (*24*). In the profile refinements, one common isotropic temperature factor was used for the metal atoms since the small number of reflections and the

large number of structural variables do not justify introduction of individual or anisotropic thermal parameters.

Low temperature magnetic susceptibility. The a.c. induction method was adopted for determination of T_c and the Meissner effect of the superconducting samples. The powdered sample (50 mg) was placed into a cylindrical ($l/r \approx \sqrt{3}$) sample holder inside a field coil (300 Hz) and cooled by liquid nitrogen. The magnetic flux density at the sample site was approximately 1 mT. The voltage induced in the sample coils was amplified by a lock-in voltmeter (EG&G, Model 5104 with a Model 5004 ultralow-noise preamplifier). The temperature was increased at a rate of 1 K/min and was measured at the sample site using a type T, Cu–Cu/Ni thermocouple. The Meissner effect was determined as an absolute value of dimensionless diamagnetic susceptibility, expressed in percents. An apparent density of 3 g/cm^3 was used to calculate the susceptibility of the powder sample per unit volume. For determination of T_c, the fairly sharp transition curves were tangentially extrapolated to zero in the vicinity of the critical point region. No more than 0.5% of the Meissner effect remained at the read value of T_c.

Results and Discussion

Homogeneity Region

Phase pure (≥99.5%) $Y(Ba_{1-y}Sr_y)_2Cu_3O_{9-\delta}$ samples are prepared within the range of solid solubility [$0.00 \leq y \leq 0.35(3)$], for the maximum firing temperature 910°C. If higher substitution levels are attempted, the superfluous strontium is bound into a mixture of $(Sr,Y)_{14}Cu_{24}O_{41}$ (*25, 26*) and $Y_2(Ba_{0.9}Sr_{0.1})CuO_5$. (The composition of the latter phase is estimated on comparison of the observed unit cell volumes of the pure and the partly Sr-substituted Y_2BaCuO_5 type phase [0.49163(3) nm^3 and 0.4888(1) nm^3, respectively] on the assumption of addivity of molar volumes for SrO and BaO in the structure.) Minor amounts of the superfluous strontium may possibly enter the Y site of the main phase, thereby in turn facilitating an even higher Sr substitution at the Ba site. This is indicated by a continued (but slight) decrease of the unit cell parameter c when the *nominal* y exceeds the 0.35(3) limit for the (purely) Y for Ba substitution and the second phases appear. The presented picture is in accordance with the scarce data in the literature, where solid solubility limits in the range of $y = 0.40$ to 0.50 are reported (*11, 13, 15, 18, 19*) for firing temperatures between 950 and 1000°C and oxygen contents of $9 - \delta = 6.70$–6.76 (*13*) or 6.92–6.95 (*19*).

If a substitution of the type $(Y_{1-x}Sr_x)Ba_2Cu_3O_{9-\delta}$ is attempted, a two-phase mixture is obtained. The Ba site is substituted instead, and the superfluous Ba and Cu form $BaCuO_{2+\nu}$. From mass balance calculations for samples with *nominal* Sr for Y substitution $x = 0.10$ and 0.20, it follows that the maximum substitution level is $x = 0.04(3)$, and that a parallel Sr for Ba substitution with $y = 0.03(1)$ and $y = 0.10(2)$, respectively, takes care of the "stoichiometry". The phase compatibilities are shown in the tetrahedral phase diagram of the Y(O)–Ba(O)–Sr(O)–Cu(O) system in Fig. 1 [including data also from Ref. (*27*)].

Under the described standard preparation conditions, the formal copper valency is virtually constant, $\nu(Cu) = 2.30(1)$, and the oxygen content is thereby independent of the degree of substitution (y).

Structural Properties and Superconductivity

The substitution of Ba^{2+} by the smaller Sr^{2+} results in shortening of all three unit cell dimensions. The contraction is anisotropic (slightly larger along the c axis), as seen from the unit cell dimensions curves in

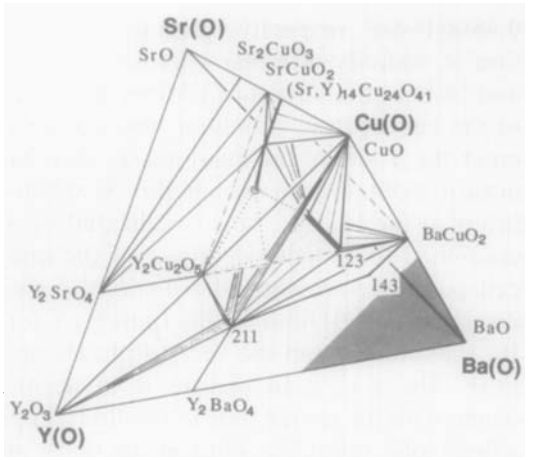

FIG. 1. Pseudoquaternary tetrahedral phase diagram of the Y(O)–Ba(O)–Sr(O)–Cu(O) system as observed for samples repeatedly fired at 910°C and saturated in oxygen at 340°C. Only the relevant portion between the solid solutions $Y(Ba_{1-y}Sr_y)_2Cu_3O_{9-\delta}$ (a), $(Sr,Y)_{14}Cu_{24}O_{41}$ (b), $Y_2(Ba,Sr)CuO_5$ (c), and CuO is drawn. Line distinctions: thick, tie line; thin, solid solution tie line; broken, pseudo-pseudoternary cut YCu(O)–Ba-Cu(O)–SrCu(O); dotted, intersections of the three-phase walls with the plane of the YCu(O)–BaCu(O)–SrCu(O) cut (three-phase "tie" lines).

Fig. 2; the least squares approximations give

$$a + b = 2[385.20(7) - 6.3(3) \cdot y]\text{pm},$$
$$c = 3[389.29(9) - 8.7(5) \cdot y]\text{pm}, \quad (1)$$

for $0.00 \leq y \leq 0.35(3)$. The tetragonal deformation of the pseudoperovskite cell[1] $D_t = [2c/3(a + b)] - 1$, decreases with y, whereas the orthorhombic deformation[2] parameter, $D_o = (b/a) - 1$, remains constant:

$$D_t = 0.0107(1) - 0.0059(7) \cdot y,$$
$$D_o = 0.0176(2) + 0.0003(10) \cdot y, \quad (2)$$

for $0.00 \leq y \leq 0.35(3)$. The nature of the contraction in the Sr case is different from that caused by the substitution of La for Ba, when a rapid decrease of D_o, a more profound contraction of c, and a virtually constant $a + b$, are observed (*7, 8*), resulting in an overall profound decrease in D_t.

The anisotropy of the contraction of the unit cell parameters upon increasing y is in qualitative agreement with an early estimate [Ref. (*11*), using only three reflections to assess a, b, c] and for later data claimed for particular "almost pure" samples with nominal $y = 0.5$ (*15, 18*). The reported (*10*) decrease in the orthorhombic deformation upon increasing y could not be confirmed, and this may be due to a higher temperature for the oxygen saturation (700°C), and the

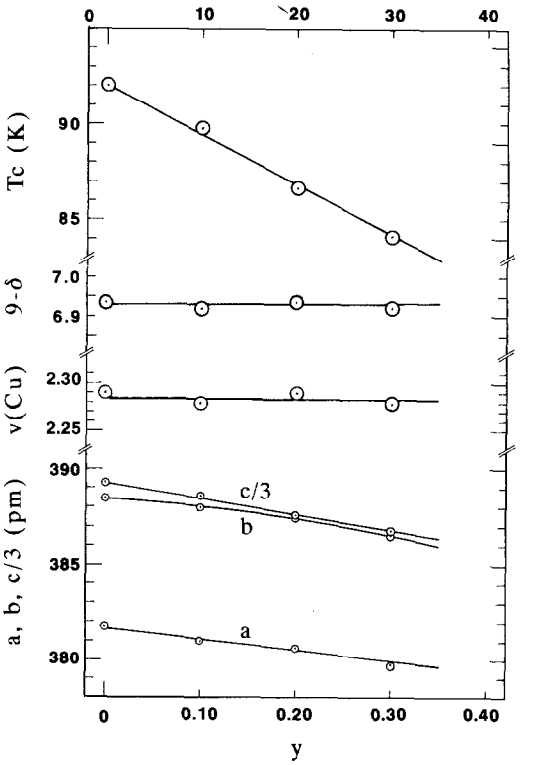

FIG. 2. Unit cell dimensions (at 297 K) as functions of strontium substitution for oxygen-saturated samples (100 kPa O_2, 340°C) of $Y(Ba_{1-y}Sr_y)_2Cu_3O_{9-\delta}$ (prepared in parallel). Oxygen content $9 - \delta$, formal Cu valency, and superconducting transition temperature T_c are also shown.

[1] As compared to the $\mathcal{O}_h$ symmetry of a single perovskite cell; calculated from the *hhl* reflections only.

[2] As compared to the $\mathcal{D}_{4h}$ symmetry of a tetragonally deformed, single perovskite cell.

fact that the vacancy concentration (*19*) and/or the temperature (*13*), which convert the structure to the tetragonal symmetry, decrease with y.

Atomic coordinates and occupancies of the oxygen sites are refined from low-temperature PND data of $Y(Ba_{1-y}Sr_y)_2Cu_3O_{6.948(6)}$. Data for $y = 0.00$, 0.10, 0.15, 0.20, and 0.30 are given in Table I. Some selected interatomic distances, listed in Table II, indicate that the contraction is centered at the Ba/Sr site, but that also shortening of Cu–O distances occurs. Such local distortions at the Ba/Sr site were recently confirmed in an EXAFS study by Zhang *et al.* (*17*). Notably, no overall contraction is observed within the Y coordination sphere (*17, 18*), Table II. In parallel with this, the average Ba/Sr–O distance shortens (by 7.7 · y pm) and the Cu–O framework contracts. Within the *ab* plane, the Cu(1)–O(1) distance decreases proportionally to b, since these atoms occupy fixed positions. An uneven contraction occurs for the O(3)–Cu(2)–O(4) sheet, which results in a further buckling of the layer, and this is in turn compensated by a significant shortening (16 · y pm) of the Cu(2)–O(2) bond. Moreover, the Rietveld refinements indicate a slight, irregular increase in the occupation of the O(5) site [with a corresponding decrease for O(1); Table I], as the unit cell shrinks due to the substitution.

A rather small, but significant, decrease in T_c is observed with increasing substitution [$0.00 \leq y \leq 0.35(3)$]:

$$T_c = 90.4(2) - 20(2) \cdot y \text{ K}. \qquad (3)$$

The Cu(1) coordination sphere is commonly considered to be a "charge reservoir" and the Cu(2) sphere to be a "pairing reservoir". The fact that the oxygen content remains constant upon the substitution strongly suggests that the overall charge confined to the copper oxygen net is conserved. However, a charge redistribution may still be controlling the decrease of T_c.

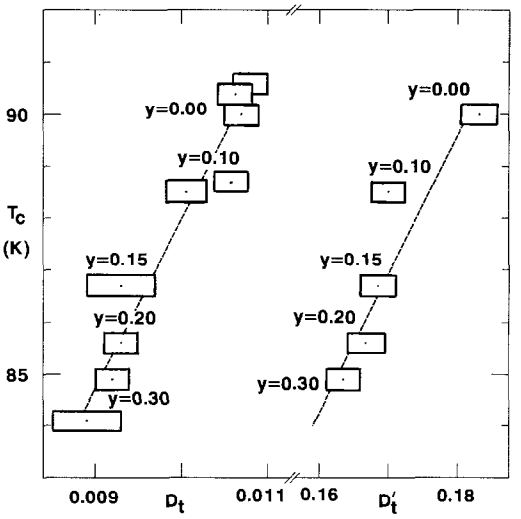

FIG. 3. T_c for $Y(Ba_{1-y}Sr_y)_2Cu_3O_{9-\delta}$ as a function of tetragonal deformation of the unit cell, ($D_t = [2c/3(a + b)] - 1$; calculated using only *hhl* PXD reflections; only a part of the samples is included in Table I) and of the apical deformation of the Cu(2) square pyramid ($D_t' = [4d_{Cu(2)-O(2)}/(a + b)] - 1$; PND data 297 K, Tables I and II). Sizes of the rectangles indicate estimated standard deviations, dashed lines are least squares fitted.

According to the slightly enhanced contraction of the crystal structure along the c axis, it is presumed that the decrease of T_c is correlated with an increasing Cu $3d_{z^2}$ component in the Cu $3d_{x^2-y^2}$ band (*28*), [or a decreased splitting of the Cu $3d_{z^2}$ and Cu $3d_{x^2-y^2}$ orbitals (*9, 29, 30*) if a crystal field model is adopted]. If the above-described anisotropic contraction is expressed in terms of the tetragonal deformation parameter D_t, a correlation with the variation in T_c is obtained (Fig. 3). Remarkably, also for various other substituted $YBa_2Cu_3O_{9-\delta}$ phases, T_c correlates with D_t (*9*). However, T_c should more properly be correlated directly with the tetragonal deformation within the Cu coordination polyhedra, rather than for the unit cell. Such correlation is indeed obtained for the Cu(2) square pyramid, and the dependence of T_c on $D_t' = [4d_{Cu(2)-O(2)}/(a + b)] - 1$ is shown in the second half of Fig. 3. (When considering

TABLE I

REFINED STRUCTURAL PARAMETERS OF $Y(Ba_{1-y}Sr_y)_2Cu_3O_{6.948(6)}$

		y:	0.00		0.10		0.15		0.20		0.30	
Variable	specification		297 K	20 K	297 K	20 K	297 K	20 K	297 K	20 K	297 K	20 K
$z_{coord.}$	Ba(Sr)	Site 2*t*	0.1793(7)	0.1782(8)	0.1793(8)	0.177(1)	0.1776(7)	0.1772(8)	0.1782(8)	0.1746(9)	0.1782(8)	0.1787(7)
$z_{coord.}$	Cu(2)	Site 2*q*	0.3568(4)	0.3568(5)	0.3558(5)	0.3575(8)	0.3565(5)	0.3552(5)	0.3562(5)	0.3559(6)	0.3550(5)	0.3549(5)
$z_{coord.}$	O(2)	Site 2*q*	0.1617(7)	0.1629(7)	0.1627(7)	0.166(1)	0.1634(7)	0.1638(7)	0.1635(7)	0.1657(8)	0.1628(7)	0.1644(7)
$z_{coord.}$	O(3)	Site 2*s*	0.3833(8)	0.3851(8)	0.3841(9)	0.388(1)	0.3858(9)	0.3855(9)	0.3851(9)	0.3865(9)	0.3838(9)	0.3855(9)
$z_{coord.}$	O(4)	Site 2*r*	0.3744(7)	0.3723(7)	0.3712(8)	0.371(1)	0.3699(8)	0.3706(8)	0.3670(8)	0.3693(9)	0.3705(8)	0.3694(8)
$n_{occup.}$	O(1)	Site 1*e*	1.00(2)	1.00(2)	0.94(2)	0.96(3)	0.85(2)	0.86(2)	0.86(2)	0.94(2)	0.88(2)	0.87(2)
$n_{occup.}$	O(5)	Site 1*b*	0.05(2)	0.06(2)	0.07(2)	0.10(3)	0.13(2)	0.14(1)	0.08(2)	0.11(2)	0.08(2)	0.12(2)
R	Nuclear		0.042	0.041	0.045	0.09	0.054	0.054	0.041	0.059	0.049	0.049
R	Profile		0.120	0.124	0.129	0.18	0.121	0.121	0.123	0.143	0.124	0.124
$9 - \delta$	Iodometry		6.954(5)		6.955(5)		6.940(5)		6.947(5)		6.946(5)	
a	Refined	(pm)	381.33(2)	380.55(2)	380.70(2)	380.06(3)	380.85(2)	380.08(2)	379.84(2)	379.23(2)	379.44(2)	378.67(2)
b	Refined	(pm)	388.00(3)	387.43(3)	387.34(4)	386.98(5)	386.75(4)	386.19(3)	386.50(3)	386.18(4)	385.79(4)	385.12(3)
c	Refined	(pm)	1165.1(1)	1161.2(1)	1162.5(1)	1158.6(2)	1160.6(1)	1156.8(1)	1159.6(1)	1155.9(1)	1157.2(1)	1153.9(1)
a	X-ray	(pm)	381.91(3)	—	381.22(4)	—	381.11(5)	—	380.58(3)	—	379.98(5)	—
b	X-ray	(pm)	388.49(3)	—	387.99(4)	—	387.72(5)	—	387.37(3)	—	386.58(5)	—
c	X-ray	(pm)	1167.9(1)	—	1165.4(1)	—	1163.0(2)	—	1162.6(1)	—	1160.0(2)	—

Note. As obtained by Rietveld refinements for (spaee group *Pmmm*) from PND data measured at 20 and 297 K. The remaining atoms are at sites fixed by symmetry: Y at 1 h, Cu(1) at 1a, O(1) at 1e, and O(5) at 1b. Occupancies of O(2), O(3), and O(4) constrained. Other constraints: isotropic thermal factors, $B = 39 \times 10^{-6}$ pm^{-2} equal for all metals, $B = 49 \times 10^{-6}$ pm^{-2} for oxygen atoms.

TABLE II

TRENDS IN INTERATOMIC DISTANCES FOR $Y(Ba_{1-y}Sr_y)_2Cu_3O_{6.948(6)}$

Atoms (i–j)	y=0.00	0.10	0.15	0.20	0.30	$\Delta d_{i-j}/y$	$d_{i-j;y=0}$
Ba–O(1)	283.4	282.8	281.0	281.3	280.8	−9(2)	283.3(5)
	282.5	280.9	280.7	278.2	281.2	−7(7)	281.7(13)
Ba–O(2)	273.2	272.7	272.3	272.1	271.6	−5.4(3)	273.2(1)
	273.0	272.2	272.3	271.7	271.5	−5(1)	272.9(2)
Ba–O(3)	307.3	307.6	310.2	308.8	307.0	±0(7)	308.1(12)
	310.0	312.8	310.3	313.4	308.1	−5(11)	311.7(20)
Ba–O(4)	297.3	293.8	293.8	290.5	293.0	−16(8)	296.1(15)
	296.4	296.2	294.8	295.7	291.6	−15(5)	297.2(10)
Ba–O(5)	285.6	285.1	283.3	283.6	283.0	−9(3)	285.5(5)
	284.7	283.2	282.9	280.6	283.4	−6(6)	283.9(12)
Cu(1)–O(1)	194.2	194.0	193.9	193.7	193.3	−3.0(3)	194.3(1)
Cu(1)–O(2)	188.9	189.6	190.0	190.1	188.8	±0(3)	189.5(6)
	190.3	194.0	190.5	192.6	190.7	±0(8)	191.7(15)
Cu(1)–O(5)	191.0	190.6	190.6	190.3	190.0	3.3(3)	191.0(1)
Cu(2)–O(2)	227.9	225.0	224.6	224.0	223.0	−16(2)	227.3(5)
	226.5	222.6	222.6	221.1	221.0	−18(5)	225.5(9)
Cu(2)–O(3)	193.4	193.4	193.6	193.2	192.9	−2(1)	193.6(2)
	193.8	193.8	193.8	193.6	193.3	−0.8(3)	193.8(1)
Cu(2)–O(4)	195.3	194.8	194.5	194.1	194.1	−4.3(8)	195.2(2)
	195.1	194.7	194.7	194.3	194.0	−3.4(6)	195.1(1)
Cu(2)–Cu(2)	334.5	336.1	333.8	334.4	336.4	+4(5)	334.4(10)
	334.5	332.1	336.8	335.1	336.6	+9(8)	333.6(15)
Y–O(3)	237.3	236.4	235.0	235.3	235.6	−6(3)	236.8(6)
	236.1	234.1	235.2	234.4	234.5	−4(3)	235.5(6)
Y–O(4)	240.8	242.6	243.3	245.2	242.2	+7(7)	241.8(13)
	242.3	242.4	242.8	243.5	243.0	+3(2)	242.3(3)

Note. All values in pm as calculated from refined atomic coordinates (PND data, 297 K upper values, 20 K lower values) and from the *room temperature* PXD unit cell dimensions. Calculated slopes (by least squares) $\Delta d_{i-j}/y$, and calculated distances at zero substitution, $d_{i-j;y=0}$ are included.

the two halves of Fig. 3, it should be born in mind that T_c vs D_t is much easier and, usually, more accurately obtained than T_c vs D_t'. The more detailed shapes of the T_c vs D_t or D_t' are subject to further studies.) A charge transfer from the Cu(1) to Cu(2) coordination sphere is indicated by the large compression of the Cu(2)–O(2) bond, compared with Cu(1)–O(2), which remains constant (see Table II). As proposed in Ref. (*31*), this charge transfer will not necessarily increase T_c, since the hole content is near optimum. Moreover, the positive effect of holes on T_c may be reversed by the earlier-discussed decrease in tetragonal deformation at Cu(2).

Deformation by Chemical and Applied Pressure

The information on the effects of high external pressures on $YBa_2Cu_3O_{9-\delta}$ are rather sparse (*31–38*). Even for the energy dispersive technique using synchrotron radiation, the resolution of the Bragg reflections for this pseudocubic phase is hardly satisfactory (*32*). Two models for the anisotropic contraction of the structure were proposed (*33*), with respectively the largest contrac-

TABLE III

COMPRESSIBILITY AND DEFORMATION OF $RE Ba_2Cu_3O_{\approx 6.95}$ UPON APPLIED AND CHEMICAL PRESSURE

Ref.	Medium	*RE*	$-\beta = \frac{1}{V_0}\left(\frac{\Delta V}{\Delta P}\right)$	$\frac{\Delta D_t}{\Delta P}$	*P* range (GPa)
(*32*)	Alcohol mix	Eu	−0.0051(5)	−0.0007(2)	0–5
(*33*)	NaF	Y	−0.0044(5)	−0.0008(2)	0–12
(*34*)	C_8H_{18}	Y	−0.0052(6)	−0.0008(2)	0–1
(*35*)	NaF	Gd	−0.0058(6)	−0.0012(2)	0–14
(*36*)	Alcohol mix	Y	−0.0078(1)	−0.0018(6)	0–11
(*37*)	He	Y	−0.0077(7)	−0.0020(4)	0–1
(*31*)	He	Y	−0.0081(1)	−0.0024(1)	0–0.6
			$-\beta_c = \frac{1}{V_0}\left(\frac{\Delta V}{\Delta y}\right)$	$\frac{\Delta D_t}{\Delta y}$	*y* range
$Y(Ba_{1-y}Sr_y)_2Cu_3O_{6.948(6)}$			−0.055(2)	−0.0059(7)	0.00–0.30

Note. β and β_c are coefficients of compressibility and chemical compressibility, respectively; $\Delta D_t/\Delta P$ and $\Delta D_t/\Delta y$ see text. Errors estimated from variation of unit cell dimensions are shown in brackets. For Ref. (*33*) major contraction along *c* is assumed. Pressure-transmitting media are listed to give a hint about the degree of hydrostatic character.

tion along *c* or *b*. Recent studies (*31*, *34–38*) support the model with the more extensive contraction along *c*. Calculated values for the compressibility β and the pressure derivatives (slopes) for the unit cell deformation $\Delta D_t/\Delta P$ are listed in Table III. Particularly for the latter, a profound diversity is noted. Characterization of the oxygen content is often missed, when comparing the ambient-pressure unit cell parameters. For the sake of comparisons with the effects of strontium substitution, the recent, time-of-flight PND study (*31*) is chosen from those in Table III. Then, assuming a volume–change equivalency between the real and the chemical (Sr substitution) pressures, a chemical pressure (P^*) coefficient $\varepsilon = P^*/y$ can be calculated as

$$\varepsilon_V = (\Delta V/\Delta y)/(\Delta V/\Delta P) = 6.8(2)\ \text{GPa}. \quad (4)$$

If one instead compares the pressure-induced changes in terms of the tetragonal deformation D_t, one obtains:

$$\varepsilon_{D_t} = (\Delta D_t/\Delta y)/(\Delta D_t/\Delta P) = 2.4(4)\ \text{GPa}. \quad (5)$$

Judged form ε_V and ε_{D_t}, the real pressure introduces a more anisotropic contraction than the Sr substitution does. This may be associated with the fact that the Y layer remains essentially unperturbed by chemical pressure (Table II). Nevertheless, an appropriate test for the chemical pressure concept is to check whether it accounts adequately for the variations in physical properties, e.g., to estimate $T_c(P)$ from ε_V and ε_{D_t}.

Superconductivity upon Chemical and Applied Pressure

Various theoretical models have been forwarded (*1*, *2*, *39*, *40*) in order to describe the response of T_c on external pressure. The pressure effects of the "classical" superconductors are discussed within the frame of the BCS theory. Recently, three simple cases, black phosphorus, PdH/PdD, and Zr_xNi_{1-x} were investigated (*41–44*), which allowed quantitative evaluation of T_c, using the Allen Dynes version (*45*) of the McMillan formula (*46*). The pressure

dependence of T_c for the high-pressure primitive cubic modification of phosphorus was found (*41*) governed by the pressure variation of a *sp* component of the electron–phonon matrix element, while the overall density of states at the Fermi level did not correlate.

The calculated (*42, 43*) T_c vs P dependence for PdH and PdD was found to be entirely determined by the pressure functions of the phonon frequencies. This is somewhat remarkable since these parameters were successfully constrained in the case of black phosphorus.

For the amorphous superconductor Zr_xNi_{1-x} (*44*), possible anisotropy effects of the crystal structure should be eliminated. A smooth change in the pressue derivative of T_c, from positive to negative, is reported (*44*) as a function of composition. Contrary to the phosphorus case (*41*), the $T_c(P)$ variation is found to be correlated with changes in the density of states at the Fermi level.

Evidently, even for the classical superconductors described by the BCS theory, no single variable in the (empirical) formulae for T_c is able to explain in a general way the response of superconductivity to applied pressure. According to Ref. (*41*), the contributions of the particular bands and their characters at the Fermi level may play the role of "primary variables". Information about the pressure variations of the (crystal) structure, particularly the anisotropy of contractions, is accordingly needed for a more comprehensive understanding. As stressed in Ref. (*40*), the pressure dependence of T_c cannot simply be expressed in terms of volume derivatives, since the pressure may act anisotropically.

This speaks for focusing on the anisotropy of the contraction(s) when comparing chemical and external pressure effects on T_c for $YBa_2Cu_3O_{9-\delta}$. An estimate of the T_c vs P slope can be obtained from combination of Eqs. (3) and (5), under an assumption of equivalence between chemical and external pressure:

$$\Delta T_c/\Delta P = (\Delta T_c/y)/\varepsilon_{D_t} \approx -8(3)\ \text{K/GPa}, \quad (6)$$

or

$$\Delta T_c/\Delta P \approx -2.9(4)\ \text{K/GPa} \quad (7)$$

if the ε_V relation in Eq. 4 is used.

However, for $YBa_2Cu_3O_{9-\delta}$ the average (external) pressure derivative of T_c is measured as positive, although rather small, $\partial T_c/\partial P = 0.70(25)$ K/GPa [Ref. (*1*); three extreme values excluded]. This significant difference in behavior between chemical and external pressure on the onset of superconductivity in $YBa_2Cu_3O_{9-\delta}$ is striking. The chemical substitution and/or the external pressure must accordingly bring unequivalent changes into the structure. Concerning the chemical substitution, a possibility is that the presence of Sr at the Ba sites causes local strain, variations of which decrease T_c via influencing the Cu–O square chains and thus affecting the distribution of charge carriers [cf. the increased occupancy of the O(5) site, vide supra and Table I]. A variable which would selectively increase T_c by the action of an external pressure is hard to imagine, although Hall effect (*47*) measurements show an increase in the hole concentration under external pressure. An estimate of the selective effect which an external pressure has on T_c for $YBa_2Cu_3O_{9-\delta}$ would be between +4 and +9 K/GPa if one assumes that one has to counterbalance the decrease in T_c which is supposed to occur upon the anisotropic unit cell contraction as signaled by the $Y(Ba_{1-y}Sr_y)_2Cu_3O_{9-\delta}$ model system. On this basis it seems more probable that the reason for the noncquivalency between chemical and external pressure is rather rooted in the properties of the $Y(Ba_{1-y}Sr_y)_2Cu_3O_{9-\delta}$ solid solution phase.

Some other oxide superconductors also have positive $T_c(P)$ slopes. The contraction of $(La,Sr)_2CuO_4$ is virtually isotropic (*48,*

49), D_t increases slightly (*50*), and $\partial T_c/\partial P = 2.1 \pm 1.5$ K/GPa (*1, 51*) is in good accordance with $T_c \approx 37$ K. A very large $\partial T_c/\partial P = 5.5 \pm 0.25$ K/GPa is reported (*52–55*) for $YBa_2Cu_4O_8$. Due to the complex anisotropic contraction for this phase (*56, 57*), comparisons with $YBa_2Cu_3O_{9-\delta}$ are not straightforward. A relevant example of the behavior of noncuprate high T_c superconductors is provided by $Ba_{1-x}K_xBiO_3$ (*3*). This cubic phase shows no anisotropy upon compression and $\partial T_c/\partial P \approx 1$ K/GPa, which corresponds well in magnitude to $T_c \approx 30$ K for this compound.

It is believed that a further elucidation of the similarities and differences between the effects of chemical and external pressure upon superconductivity can be obtained experimentally, and an investigation of chemical pressure effects in $YBa_2Cu_4O_8$ is in progress.

Acknowledgment

This work has received financial support from the Norwegian Council for Science and the Humanities (NAVF).

References

1. R. J. WIJNGAARDEN, AND R. GRIESSEN, *in* "Studies of High Temperature Superconductors, Advances in Research and Applications" (A. V. Narlikar, Ed.), Vol. 2, Nova Science Publishers, New York. pp 29–77 (1989).
2. R. GRIESSEN, *Phys. Rev. B: Condens. Matter* **36,** 5284 (1987).
3. J. E. SCHIRBER, P. MOROSIN, AND D. S. GINLEY, *Physica C (Amsterdam)* **157,** 237 (1989).
4. B. BUCHER, J. KARPINSKI, E. KALDIS, AND P. WACHTER, *Physica C (Amsterdam)* **157,** 478 (1989).
5. P. KAREN, H. FJELLVÅG, O. BRAATEN, A. KJEKSHUS, AND H. BRATSBERG, *Acta Chem. Scand.* **44,** 994 (1990).
6. H. FJELLVÅG, P. KAREN, A. KJEKSHUS, AND A. F. ANDRESEN, *Physica C (Amsterdam)* **162–164,** 49 (1989).
7. A. F. ANDRESEN, H. FJELLVÅG, P. KAREN, AND A. KJEKSHUS, *Z. Kristollogr.* **185,** A2 (1988).
8. P. KAREN, H. FJELLVÅG, A. KJEKSHUS, AND A. F. ANDRESEN, submitted for publication.
9. P. KAREN, H. FJELLVÅG, AND A. KJEKSHUS, submitted for publication.
10. B. W. VEAL, W. K. KWOK, A. UMEZAWA, G. W. CRABTREE, J. D. JORGENSEN, J. W. DOWNEY, L. J. NOVICKI, A. W. MITCHELL, A. P. PAULIKAS, AND H. C. SOWERS, *Appl. Phys. Lett.* **51,** 279 (1987).
11. T. WADA, S. ADACHI, T. MIHARA, AND R. INABA, *Jpn. J. Appl. Phys., Part 2* **26,** L706 (1987).
12. T. WADA, S. ADACHI, O. INOUE, S. KAWASHIMA, AND T. MIHARA, *Jpn. J. Appl. Phys., Part 2* **26,** L1475 (1987).
13. A. ONO, T. TANAKA, H. NOZAKI, AND Y. ISHIZAWA, *Jpn. J. Appl. Phys., Part 2* **26,** L1687 (1987).
14. Y. ZHAO, H. ZHANG, T. ZHANG, S. F. SUN, Z. Y. CHEN, AND Q. R. ZHANG, *Physica C (Amsterdam)* **152,** 513 (1988).
15. H. M. SUNG, J. H. KUNG, J. M. LIANG, R. S. LIU, Y. C. CHEN, P. T. WU, AND L. J. CHEN, *Physica C (Amsterdam)* **153–155,** 866 (1988).
16. J. M. LIANG, L. CHANG, H. M. SUNG, P. T. WU, AND L. J. CHEN, *J. Appl. Phys.* **64,** 3593 (1988).
17. K. ZHANG, G. BUNKER, B. CHANCE, AND C. F. GALLO, *Phys. Rev. B: Condens. Matter* **39,** 2788 (1989).
18. Y. MATSUDA, M. YOSHIDA, AND S. HINOTANI, *Jpn. J. Appl. Phys., Part 2* **28,** L1128 (1989).
19. K. FUEKI, Y. IDEMOTO, AND H. ISHIZUKA, *Physica C (Amsterdam)* **166,** 261 (1990).
20. P. E. WERNER, The Computer Programme SCANPI, Institute of Inorganic Chemistry, University of Stockholm, Sweden (1981).
21. N. O. ERSSON Programme CELLKANT, Chemical Institute, Uppsala University, Uppsala, Sweden (1981).
22. H. M. RIETVELD, *J. Appl. Crystallogr.* **1,** 65 (1968).
23. A. W. HEWAT, *UKAERE Harwell Rep.* RRL 73/897 (1973).
24. L. KOESTER, AND W. B. YELON, *in* Neutron Diffraction Newsletter, (W. B. Yelon, Ed.) The Neutron Diffraction Commission, Missouri, (1983).
25. E. M. MCCARRON, M. A. SUBRAMANIAN, J. C. CALABRESE, AND R. L. HARLOW, *Mater. Res. Bull.* **23,** 1355 (1988).
26. M. W. MCELFRESH, J. M. D. COEY, P. STROBEL, AND S. VON MOLNAR, *Phys. Rev. B: Condens. Matter* **40,** 825 (1989).
27. D. M. DELEEUW, C. A. H. A. MUTSAERS, G. P. J. GEELEN, H. C. A. SMOORENBURG, AND C. LANGEREIS, *Physica C (Amsterdam)* **152,** 508 (1988).

28. A. MANTHIRAM, X. X. TANG, AND J. B. GOODENOUGH, *Phys. Rev. B: Condens. Matter* **42,** 138 (1990).
29. T. NAKAMURA, AND R. LIANG, *Jpn. J. Appl. Phys., Part 2* **26,** 678 (1987).
30. D. M. NEWNS, M. RASOLT, AND P. C. PATTNAIK, *Phys. Rev. B: Condens. Matter* **38,** 6513 (1988).
31. J. D. JORGENSEN, S. PEI, D. G. HINKS, B. W. VEAL, B. DĄBROVSKI, A. P. PAULIKAS, R. KLEB, AND I. D. BROWN, *Physica C (Amsterdam)* **171,** 93 (1990).
32. J. S. OLSEN, S. STEENSTRUP, I. JOHANNSEN, AND L. GERWARD, *Z. Phys. B, Condens. Matter* **72,** 165 (1988).
33. W. H. FIETZ, M. R. DIETRICH, AND J. ECKE, *Z. Phys. B, Condens. Matter* **69,** 17 (1987).
34. C. CAREL, J.-R. GAVARRI, C. PERRIN, O. PEÑA, AND C. VETTIER, *C. R. Acad. Sci., Ser. 2* **309,** 1889 (1989).
35. J. ECKE, W. H. FIETZ, M. R. DIETRICH, C. A. WASSILEW, H. WÜHL, AND R. FLÜKIGER, *Physica C (Amsterdam)* **153–155,** 954 (1988).
36. M. J. AKHTAR, Z. N. AKHTAR, AND C. R. A. CATLOW, *J. Phys.: Condens. Matter* **2,** 3231 (1990).
37. I. V. ALEKSANDROV, A. F. GONCHAROV, AND S. M. STISHOV *Sov. Phys., JETP Lett.* **47,** 428 (1988).
38. N. V. JAYA, S. NATARAJAN, AND G. V. S. RAO, *Solid State Commun.* **67,** 51 (1988).
39. T. KANEKO, H. YOSHIDA, S. ABE, H. MORITA, K. NOTO, AND H. FUJIMORI, *Jpn. J. Appl. Phys., Part 2* **26,** 1374 (1987).
40. J. M. BESSON, *J. Phys. (Paris)* **50,** 1433 (1989).
41. M. RAJAGOPALAN, M. ALOUANI, AND N. E. CHRISTENSEN, *J. Low Temp. Phys.* **75,** 1 (1989).
42. H. HEMMES, A. DRIESSEN, R. GRIESSEN, AND M. GUPTA, *Phys. Rev. B: Condens. Matter* **39,** 4110 (1989).
43. R. GRIESSEN, H. HEMMES, A. DRIESSEN, AND R. J. WIJNGAARDEN, *Z. Phys. Chem.* **163,** 695 (1989).
44. F. MAHINI, F. S. RAZAVI, AND Z. ALTOUNIAN, *Phys. Rev. B: Condens. Matter* **39,** 4677 (1989).
45. P. B. ALLEN, AND R. C. DYNES, *Phys. Rev. B: Condens. Matter* **12,** 905 (1975).
46. W. L. MCMILLAN, *Phys. Rev.* **167,** 331 (1968).
47. T. HIRAOKA, *Jpn. J. Appl. Phys., Part 2* **28,** L1135 (1989).
48. H. TAKAHASHI, C. MURAYAMA, S. YOMO, N. MORI, K. KISHIO, K. KITAZAWA, AND K. FUEKI, *Jpn. J. Appl. Phys., Part 2* **26,** 504 (1987).
49. W. H. FIETZ, C. A. WASSILEW, D. EVERT, M. R. DIETRICH, AND H. WÜHL, *Phys. Lett. A* **142,** 300 (1989).
50. S. PEI, J. D. JORGENSEN, D. G. HINKS, B. DĄBROVSKI, P. LIGHTFOOT, AND D. R. RICHARDS, *Physica C (Amsterdam)* **169,** 179 (1990).
51. N. TANAHASHI, Y. IYE, T. TAMEGAI, C. MURAYAMA, N. MORI, S. YOMO, N. OKAZAKI, AND K. KITAZAWA, *Jpn. J. Appl. Phys., Part 2* **28,** L762 (1989).
52. B. BUCHER, J. KARPINSKI, E. KALDIS, AND P. WACHTER, *Physica C (Amsterdam)* **157,** 478 (1989).
53. Y. YAMADA, T. MATSUMOTO, Y. KAIEDA, AND N. MORI, *Jpn. J. Appl. Phys., Part 2* **29,** L250 (1990).
54. J. L. TALLON AND J. LUSK, *Physica C (Amsterdam)* **167,** 236 (1990).
55. E. N. VAN EENIGE, R. GRIESSEN, R. J. WIJNGAARDEN, J. KARPINSKI, E. KALDIS, S. RUSIECKI, AND E. JILEK, *Physica C (Amsterdam)* (preprint).
56. E. KALDIS, P. FISCHER, A. W. HEWAT, E. A. HEWAT, J. KARPINSKI, AND S. RUSIECKI, *Physica C (Amsterdam)* **159,** 668 (1989).
57. H. A. LUDWIG, W. H. FIETZ, M. R. DIETRICH, H. WÜHL, J. KARPINSKI, E. KALDIS, AND S. RUSIECKI, *Physica C (Amsterdam)* **167,** 335 (1990).